

Brønsted Acid-Promoted C–H Bond Cleavage via Electron Transfer from Toluene Derivatives to a Protonated Nonheme Iron(IV)-Oxo Complex with No Kinetic Isotope Effect

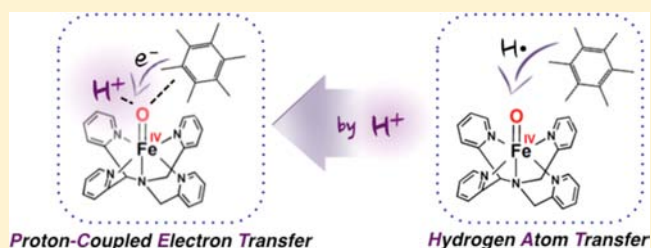
Jiyun Park,[†] Yong-Min Lee,[‡] Wonwoo Nam,^{*,‡} and Shunichi Fukuzumi^{*,†,‡}

[†]Department of Material and Life Science, Graduate School of Engineering, ALCA, Japan Science and Technology Agency, Osaka University, Suita, Osaka 565-0871, Japan

[‡]Department of Bioinspired Science, Ewha Womans University, Seoul 120-750, Korea

S Supporting Information

ABSTRACT: The reactivity of a nonheme iron(IV)-oxo complex, [(N4Py)Fe^{IV}(O)]²⁺ (N4Py = *N,N*-bis(2-pyridylmethyl)-*N*-bis(2-pyridyl)methylamine), was markedly enhanced by perchloric acid (70% HClO₄) in the oxidation of toluene derivatives. Toluene, which has a high one-electron oxidation potential ($E_{\text{ox}} = 2.20$ V vs SCE), was oxidized by [(N4Py)Fe^{IV}(O)]²⁺ in the presence of HClO₄ in acetonitrile (MeCN) to yield a stoichiometric amount of benzyl alcohol, in which [(N4Py)Fe^{IV}(O)]²⁺ was reduced to [(N4Py)Fe^{III}(OH₂)]³⁺. The second-order rate constant (k_{obs}) of the oxidation of toluene derivatives by [(N4Py)Fe^{IV}(O)]²⁺ increased with increasing concentration of HClO₄, showing the first-order dependence on [HClO₄]. A significant kinetic isotope effect (KIE) was observed when mesitylene was replaced by mesitylene-*d*₁₂ in the oxidation with [(N4Py)Fe^{IV}(O)]²⁺ in the absence of HClO₄ in MeCN at 298 K. The KIE value drastically decreased from KIE = 31 in the absence of HClO₄ to KIE = 1.0 with increasing concentration of HClO₄, accompanied by the large acceleration of the oxidation rate. The absence of KIE suggests that electron transfer from a toluene derivative to the protonated iron(IV)-oxo complex ([[(N4Py)Fe^{IV}(OH)]³⁺) is the rate-determining step in the acid-promoted oxidation reaction. The detailed kinetic analysis in light of the Marcus theory of electron transfer has revealed that the acid-promoted C–H bond cleavage proceeds via the rate-determining electron transfer from toluene derivatives to [(N4Py)Fe^{IV}(OH)]³⁺ through formation of strong precursor complexes between toluene derivatives and [(N4Py)Fe^{IV}(OH)]³⁺.



INTRODUCTION

High-valent iron-oxo complexes with heme and nonheme ligands play pivotal roles as reactive intermediates in biological and chemical oxidation reactions.^{1,2} Extensive efforts have been devoted to synthesize various nonheme iron(IV)-oxo complexes, which were characterized by various spectroscopic methods and X-ray crystallography.^{3–13} Over the past several decades, the reactivities of the biomimetic iron(IV)-oxo complexes have been investigated in various oxidation reactions such as oxygen atom transfer and C–H bond cleavage.^{7–17} It has been demonstrated that the reactivities of iron(IV)-oxo complexes are affected by supporting and axial ligands, solvents and other various reaction conditions.^{8–17} Understanding factors that control the reactivity of nonheme iron complexes in oxidation reactions are indispensable in designing efficient biomimetic catalysts with high reactivity and selectivity. One important factor that controls the reactivity of iron(IV)-oxo complexes is Brønsted acids, which can protonate iron(IV)-oxo complexes to enhance the reactivity.¹⁸

We have previously reported that Brønsted acids promote oxygen atom transfer from a nonheme iron(IV)-oxo complex and also electron transfer from one-electron reductants such as

ferrocene derivatives.^{18,19} With regard to C–H bond cleavage, nonheme iron(IV)-oxo complexes reported to date are capable of activating weak C–H bonds of activated alkanes (e.g., alkylaromatics such as xanthene, 9,10-dihydroanthracene, and fluorene).¹⁵ In the presence of Sc(OTf)₃ (OTf[−] = triflate anion), a nonheme iron(IV)-oxo complex becomes capable of oxidizing benzyl alcohol derivatives with electron-donating substituents via outer-sphere electron transfer from the benzyl alcohol derivatives to a nonheme iron(IV)-oxo complex, which is coupled with binding of Sc(OTf)₃.²⁰ In such an outer-sphere electron-transfer pathway, the reactivity of nonheme iron(IV)-oxo complexes is determined by the one-electron reduction potentials when no further enhancement of the reactivity is possible because interactions between substrates and Sc³⁺ ion-bound iron(IV)-oxo complexes are prohibited due to the steric effect of Sc³⁺ ion.²¹ In contrast to the case of Sc³⁺ ion-coupled electron transfer reactions of nonheme iron(IV)-oxo complexes, it is possible to have strong interactions between substrates and protonated nonheme iron(IV)-oxo complexes in

Received: November 29, 2012

Published: March 25, 2013

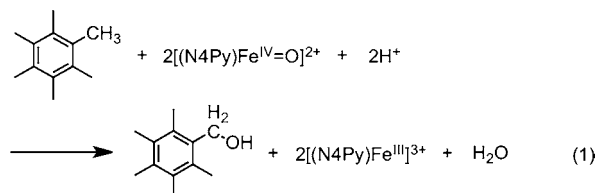
proton-coupled electron-transfer (PCET) reactions.¹⁹ However, C–H bond cleavage via PCET from substrates to nonheme iron(IV)-oxo complexes has yet to be reported.

We report herein remarkable acceleration effects of Brønsted acid (i.e., HClO₄) on C–H bond cleavage of toluene derivatives by a nonheme iron(IV)-oxo complex, [(N4Py)-Fe^{IV}(O)]²⁺ (N4Py = *N,N*-bis(2-pyridylmethyl)-*N*-bis(2-pyridyl)methylamine), via electron transfer from toluene derivatives to a protonated iron(IV)-oxo complex, [(N4Py)-Fe^{IV}(OH)]³⁺. Strong precursor complexes were formed between toluene derivatives and [(N4Py)Fe^{IV}(OH)]³⁺ prior to electron transfer. Although C–H bond cleavage of mesitylene with [(N4Py)Fe^{IV}(O)]²⁺ without HClO₄ is sluggish to exhibit a significant deuterium kinetic isotope effect (KIE = 31), the rate of C–H bond cleavage with [(N4Py)Fe^{IV}(O)]²⁺ is 10³-fold faster in the presence of HClO₄ (10 mM) to show no KIE (KIE = 1.0). The rate constants of C–H bond cleavage of toluene derivatives with [(N4Py)Fe^{IV}(O)]²⁺ and [(N4Py)-Fe^{IV}(OH)]³⁺ are quantitatively compared with those of outer-sphere electron-transfer reactions from coordinatively saturated metal complexes (one-electron reductants) to [(N4Py)-Fe^{IV}(OH)]³⁺ in light of the Marcus theory of electron transfer. The present study provides valuable mechanistic insights into the switch of the C–H bond cleavage mechanism from hydrogen atom transfer from toluene derivatives to [(N4Py)-Fe^{IV}(O)]²⁺ in the absence of HClO₄ to electron transfer from toluene derivatives to [(N4Py)Fe^{IV}(OH)]³⁺ in the presence of HClO₄.

RESULTS AND DISCUSSION

Brønsted Acid-Promoted C–H Bond Cleavage of Toluene Derivatives by [(N4Py)Fe^{IV}(O)]²⁺ with HClO₄

Although oxidation of hexamethylbenzene by [(N4Py)-Fe^{IV}(O)]²⁺ in acetonitrile (MeCN) is sluggish, the reaction with HClO₄ (10 mM) occurred efficiently to afford pentamethylbenzyl alcohol as the sole oxidized product, when [(N4Py)Fe^{IV}(O)]²⁺ was reduced to yield [(N4Py)Fe^{III}] as indicated by the EPR spectrum [Figure S1 in Supporting Information (SI)]. The stoichiometry of the oxidation of hexamethylbenzene by [(N4Py)Fe^{IV}(O)]²⁺ with HClO₄ is given by eq 1. In such a case the observed 50% yield of



pentamethylbenzyl alcohol (Figure S2 in SI) indicates the quantitative conversion because [(N4Py)Fe^{IV}(O)]²⁺ in the presence of HClO₄ acts as a one-electron oxidant without oxygen in contrast to the case in the absence of HClO₄.^{15,22–24} No further oxidation of pentamethylbenzyl alcohol was observed. The one-electron oxidation potential of pentamethylbenzyl alcohol in the presence of an acid in MeCN is higher than that of hexamethylbenzene (1.49 V vs SCE).²⁰ Thus, PCET from pentamethylbenzyl alcohol to [(N4Py)-Fe^{IV}(O)]²⁺ is expected to be slower than that from hexamethylbenzene as discussed later. In addition, much excess hexamethylbenzene relative to [(N4Py)Fe^{IV}(O)]²⁺ was employed to analyze the product. This is the reason why no

further oxidation of pentamethylbenzyl alcohol was observed in this study.

In the presence of HClO₄ (10 mM), the one-electron reduction potential of [(N4Py)Fe^{IV}(O)]²⁺ is reported to be shifted to a positive direction from 0.51 V vs SCE to 1.43 V vs SCE,^{18,19,25} which is much more positive than the one-electron oxidation potential of [(N4Py)Fe^{II}(MeCN)]²⁺ (*E*_{ox} = 1.00 V vs SCE).²⁶ Thus, [(N4Py)Fe^{II}(MeCN)]²⁺ is oxidized by [(N4Py)-Fe^{IV}(O)]²⁺ in the presence of HClO₄ to produce [(N4Py)-Fe^{III}] (Figure S1 in SI).

Rates of oxidation of toluene derivatives by [(N4Py)-Fe^{IV}(O)]²⁺ were remarkably enhanced by the presence of HClO₄. A typical example is shown in Figure 1, where the

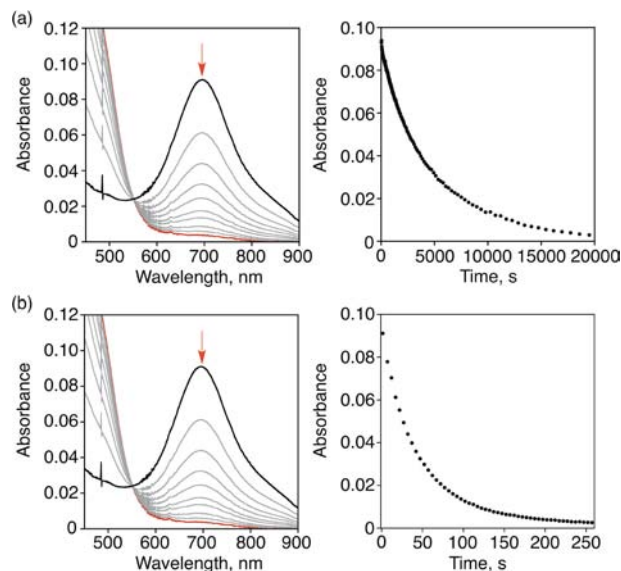


Figure 1. Visible spectral changes observed in the reaction of [(N4Py)Fe^{IV}(O)]²⁺ (0.25 mM) with 1,2,4,5-Tetramethylbenzene (TMB) ((a) 25 mM and (b) 6.3 mM) in the absence (a) and presence (b) of HClO₄ (10 mM) in MeCN at 298 K (left panel). Right panels show time courses monitored at 695 nm due to the decay of [(N4Py)Fe^{IV}(O)]²⁺.

absorption band at 695 nm due to [(N4Py)Fe^{IV}(O)]²⁺ decays in the course of oxidation of 1,2,4,5-tetramethylbenzene (TMB) by [(N4Py)Fe^{IV}(O)]²⁺. The decay rate of [(N4Py)-Fe^{IV}(O)]²⁺ becomes much faster in the presence of HClO₄ (10 mM) (Figure 1a vs b).

Decay rates of [(N4Py)Fe^{IV}(O)]²⁺ with large excess of TMB in the absence and presence of large excess HClO₄ obeyed pseudo-first-order kinetics. The pseudo-first-order rate constant increased proportionally with increasing TMB concentration (see Figure S3 in SI). The second-order rate constant (*k*_{obs}) was determined from the slope of the linear plot of the pseudo-first-order rate constant vs TMB concentration. The observed second-order rate constant (*k*_{obs}) increased linearly with increasing HClO₄ concentration (Figure 2). The *k*_{obs} values of other toluene derivatives also exhibited linear correlations with HClO₄ concentration as given by eq 2, where *k*₀ is the rate

$$k_{\text{obs}} = k_0 + k_1[\text{HClO}_4] \quad (2)$$

constant in the absence of HClO₄. A similar correlation between the rate constant of PCET from the excited state of [Ru(bpy)₃]²⁺ to aromatic carbonyl compounds and [HClO₄]

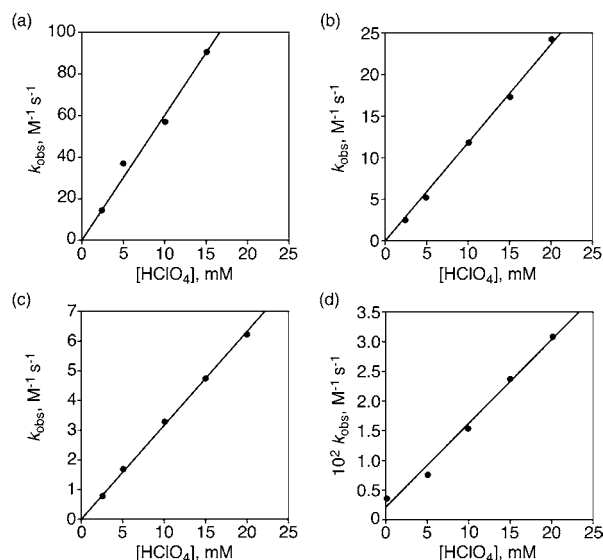


Figure 2. Plots of k_{obs} vs HClO_4 concentration in oxidation of (a) hexamethylbenzene, (b) 1,2,3,4,5-pentamethylbenzene, (c) 1,2,4,5-tetramethylbenzene and (d) 1,3,5-trimethylbenzene with $[(\text{N}4\text{Py})\text{Fe}^{\text{IV}}(\text{O})]^{2+}$ in the presence of HClO_4 in MeCN at 298 K.

has been established by using 70 wt % HClO_4 in MeCN.²⁷ The PCET rate constants are known to decrease significantly by the addition of water at constant $[\text{HClO}_4]$.²⁸ Although the k_{obs} values for oxidation of 1,2,4,5-tetramethylbenzene with $[\text{Fe}^{\text{IV}}(\text{O})(\text{N}4\text{Py})]^{2+}$ in the presence of 10 mM and 20 mM of HClO_4 (70%) in MeCN at 298 K decrease significantly with increasing added H_2O concentration, the ratio of k_{obs} with 20 mM vs 10 mM remains constant (two) irrespective of added H_2O concentration (Figure S4 in SI). This indicates that the acidity of HClO_4 (70%) decreases with increasing added H_2O but that the k_{obs} values are proportional to concentration of HClO_4 (70%) irrespective of added H_2O concentration. If we could use HClO_4 (100%), the acidity would be much higher. However, HClO_4 without H_2O may explode. Thus, we have used HClO_4 (70%) in this study to utilize the high acidity safely. We have also confirmed that the k_{obs} values of oxidation of 1,2,4,5-tetramethylbenzene with $[\text{Fe}^{\text{IV}}(\text{O})(\text{N}4\text{Py})]^{2+}$ both in the absence and presence of 10 mM of HClO_4 remain constant irrespective of concentration of tetra-*n*-butylammonium perchlorate (TBAP) as shown in Figure S5 in SI. This indicates that the ionic strength does not affect the k_{obs} values.

The observed second-order rate constants (k_{obs}) of C–H bond cleavage of toluene derivatives with $[(\text{N}4\text{Py})\text{Fe}^{\text{IV}}(\text{O})]^{2+}$ in the absence and presence of HClO_4 (10 mM) are listed in

Table 1. The k_{obs} values in the presence of HClO_4 (10 mM) relative to those in the absence of HClO_4 increase with increasing the number of methyl groups on benzene, and the enhancement is as large as 10^3 -fold in the case of hexamethylbenzene.

In the absence of HClO_4 , C–H bond cleavage of toluene derivatives with $[(\text{N}4\text{Py})\text{Fe}^{\text{IV}}(\text{O})]^{2+}$ proceeds via the rate-determining hydrogen atom transfer from toluene derivatives to $[(\text{N}4\text{Py})\text{Fe}^{\text{IV}}(\text{O})]^{2+}$. It was evidenced by observation of a large deuterium kinetic isotope effect (KIE) as shown in Figure 3a,

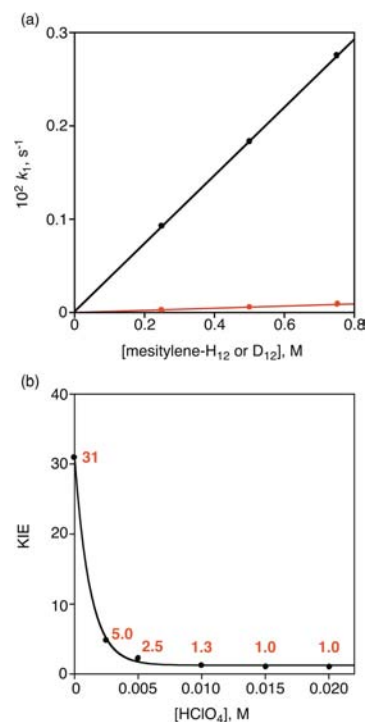


Figure 3. (a) Plots of first-order rate constants vs concentration of mesitylene in oxidation of mesitylene (black circle) and mesitylene- d_{12} (red circle) with $[(\text{N}4\text{Py})\text{Fe}^{\text{IV}}(\text{O})]^{2+}$ (0.25 mM) in the absence of HClO_4 in MeCN at 298 K. (b) Plot of KIE vs concentration of HClO_4 in MeCN at 298 K. Red numbers show the KIE values obtained experimentally.

where the rate constant of mesitylene (1,3,5-trimethylbenzene) is about 30 times larger than that of fully deuterated mesitylene (KIE = 31). Such a large KIE value suggests that the hydrogen atom transfer occurs via tunneling.^{29–32}

Table 1. One-Electron Oxidation Potentials (E_{ox}) of Toluene Derivatives and Second-Order Rate Constants of the C–H Bond Cleavage by $[(\text{N}4\text{Py})\text{Fe}^{\text{IV}}(\text{O})]^{2+}$ in the Presence of HClO_4 (10 mM) in MeCN at 298 K

toluene derivative	E_{ox} (vs SCE, V) ^a	k_{obs} $\text{M}^{-1} \text{s}^{-1}$	
		without HClO_4	with HClO_4 (10 mM)
hexamethylbenzene	1.49	$(5.1 \pm 0.2) \times 10^{-2}$	$(5.7 \pm 0.2) \times 10$
1,2,3,4,5-pentamethylbenzene	1.58	$(1.0 \pm 0.1) \times 10^{-2}$	$(1.2 \pm 0.1) \times 10$
1,2,4,5-tetramethylbenzene	1.63	$(9.8 \pm 0.4) \times 10^{-3}$	3.3 ± 0.2
1,2,4-trimethylbenzene	1.79	$(5.5 \pm 0.2) \times 10^{-3}$	$(1.9 \pm 0.1) \times 10^{-1}$
1,4-dimethylbenzene	1.93	$(4.0 \pm 0.1) \times 10^{-3}$	$(1.6 \pm 0.1) \times 10^{-2}$
1,3,5-trimethylbenzene	1.98	$(3.7 \pm 0.1) \times 10^{-3}$	$(1.6 \pm 0.2) \times 10^{-2}$
toluene	2.20	$(1.5 \pm 0.1) \times 10^{-4}$	$(5.3 \pm 0.2) \times 10^{-4}$

^aTaken from ref 33.

In the presence of HClO_4 , the k_{obs} value of oxidation of mesitylene with $[(\text{N4Py})\text{Fe}^{\text{IV}}(\text{O})]^{2+}$ increased with increasing concentration of HClO_4 (Figure 2d). However, the KIE value decreased significantly with increasing concentration of HClO_4 as shown in Figure 3b, where the large KIE value of 31 in the absence of HClO_4 is changed to no KIE (KIE = 1.0) in the presence of large concentrations of HClO_4 (>10 mM). The absence of KIE in the presence of HClO_4 (>10 mM) indicates the change of the mechanism from a rate-determining hydrogen atom transfer pathway in the absence of HClO_4 (eq 3) to an electron-transfer pathway from toluene derivatives to the monoprotonated iron(IV)-oxo complex ($[(\text{N4Py})\text{Fe}^{\text{IV}}(\text{OH})]^{3+}$) in the presence of HClO_4 (eq 4).

The change in the KIE values in the presence of HClO_4 was also observed in the oxidation reaction of toluene vs toluene- d_8 as shown in Figure 4. The large KIE value (31) in the absence

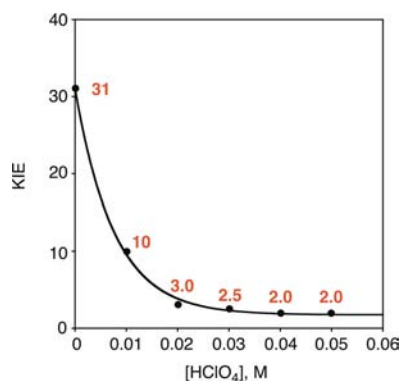
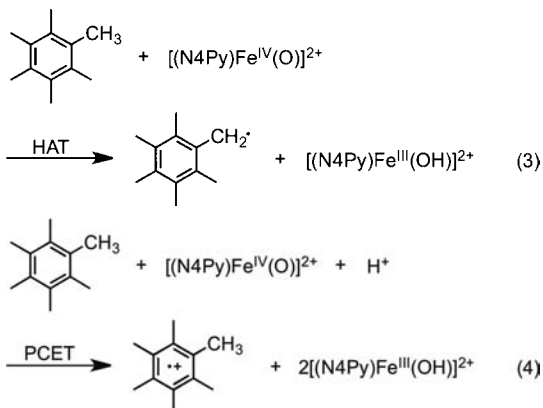


Figure 4. Plot of KIE vs concentration of HClO_4 in oxidation reaction of toluene and toluene- d_8 with $[(\text{N4Py})\text{Fe}^{\text{IV}}(\text{O})]^{2+}$ (0.25 mM) in MeCN at 298 K. Red numbers show the KIE values obtained experimentally.

of HClO_4 decreased with increasing concentration of HClO_4 . In this case, however, a small KIE value (2.0) was observed in the presence of large excess HClO_4 . This indicates that an hydrogen atom transfer pathway (eq 3) is still competing with an electron-transfer pathway from toluene to the monoprotonated iron(IV)-oxo complex ($[(\text{N4Py})\text{Fe}^{\text{IV}}(\text{OH})]^{3+}$) in the presence of HClO_4 (eq 4) under the conditions in Figure 4.



In the presence of HClO_4 , PCET from toluene derivatives to $[(\text{N4Py})\text{Fe}^{\text{IV}}(\text{OH})]^{3+}$ may become much faster than the hydrogen atom transfer reaction. Radical cations of toluene derivatives are known to undergo rapid deprotonation, producing benzyl radical derivatives, which may react with $[(\text{N4Py})\text{Fe}^{\text{IV}}(\text{O})]^{2+}$ with H^+ to yield benzyl alcohol derivatives

and $[(\text{N4Py})\text{Fe}^{\text{III}}]^{3+}$ to be consistent with the stoichiometry in eq 1. The more detailed mechanism of C–H bond cleavage of toluene derivatives with $[(\text{N4Py})\text{Fe}^{\text{IV}}(\text{O})]^{2+}$ in the presence of HClO_4 is discussed after comparison of the reactivity with that of outer-sphere PCET reactions of $[(\text{N4Py})\text{Fe}^{\text{IV}}(\text{O})]^{2+}$ (vide infra).

Outer-Sphere PCET Reactions of $[(\text{N4Py})\text{Fe}^{\text{IV}}(\text{O})]^{2+}$. In order to compare the reactivity of C–H bond cleavage reactions, which proceed via PCET of toluene derivatives with $[(\text{N4Py})\text{Fe}^{\text{IV}}(\text{OH})]^{3+}$, the reactivity of outer-sphere PCET reactions of $[(\text{N4Py})\text{Fe}^{\text{IV}}(\text{OH})]^{3+}$ was examined using coordinatively saturated metal complexes, $[\text{Fe}^{\text{II}}(\text{Me}_2\text{bpy})_3]^{2+}$ (Me_2bpy = 4,4'-dimethyl-2,2'-bipyridine), $[\text{Ru}^{\text{II}}(\text{Me}_2\text{bpy})_3]^{2+}$, $[\text{Fe}^{\text{II}}(\text{Clphen})_3]^{2+}$ (Clphen = 5-chloro-1,10-phenanthroline) and $[\text{Ru}^{\text{II}}(\text{Clphen})_3]^{2+}$, as electron donors.¹⁹ In contrast to the case of PCET reactions of $[(\text{N4Py})\text{Fe}^{\text{IV}}(\text{OH})]^{3+}$ with toluene derivatives as shown in Figure 2, where the second-order rate constants (k_{obs}) show linear correlations with $[\text{HClO}_4]$, the k_{obs} values of PCET reactions of $[(\text{N4Py})\text{Fe}^{\text{IV}}(\text{OH})]^{3+}$ with coordinatively saturated metal complexes show the first-order dependence on $[\text{HClO}_4]$ at lower concentrations that changes to the second-order dependence on $[\text{HClO}_4]$ at higher concentrations (Figure 5). Such mixture

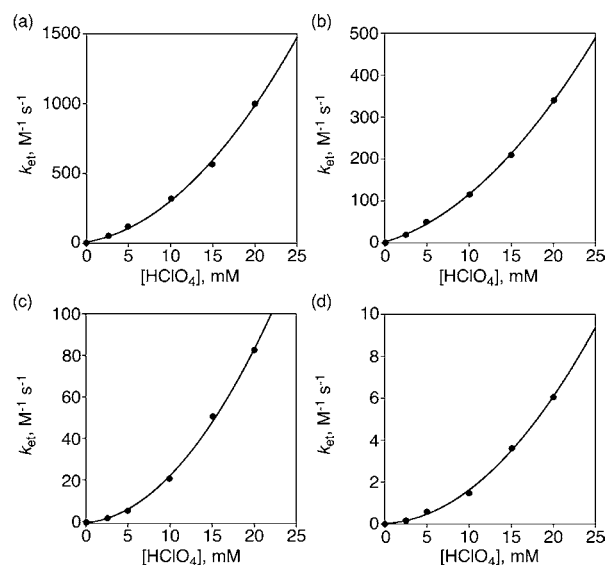


Figure 5. Plots of k_{et} vs concentration of HClO_4 in PCET from (a) $[\text{Fe}^{\text{II}}(\text{Me}_2\text{bpy})_3](\text{PF}_6)_2$, (b) $[\text{Ru}^{\text{II}}(\text{Me}_2\text{bpy})_3](\text{PF}_6)_2$, (c) $[\text{Fe}^{\text{II}}(\text{Clphen})_3](\text{PF}_6)_2$ and (d) $[\text{Ru}^{\text{II}}(\text{Clphen})_3](\text{PF}_6)_2$ to $[(\text{N4Py})\text{Fe}^{\text{IV}}(\text{O})]^{2+}$ in the presence of HClO_4 (70%) in MeCN at 298 K.

of the first- and second-order dependence of k_{obs} on $[\text{HClO}_4]$ is given by eq 5,

$$k_{\text{obs}} = k'_0 + k'_1[\text{HClO}_4] + k'_2[\text{HClO}_4]^2 \quad (5)$$

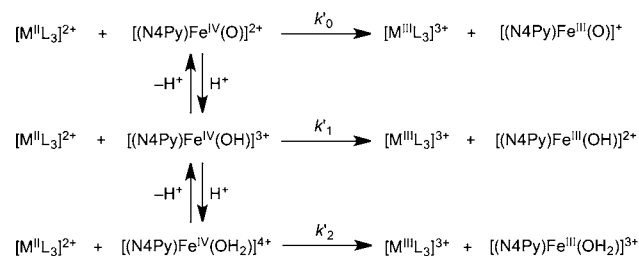
where k'_0 , k'_1 and k'_2 are the rate constants for the zero-, first- and second-order dependence on $[\text{HClO}_4]$, respectively. Because the k'_0 value in the absence of HClO_4 is negligible as compared with k'_1 and k'_2 , eq 5 is rewritten by eq 6,

$$k_{\text{obs}}/[\text{HClO}_4] = k'_1 + k'_2[\text{HClO}_4] \quad (6)$$

which predicts a linear correlation between $k_{\text{obs}}/[\text{HClO}_4]$ vs $[\text{HClO}_4]$. Linear plots of $k_{\text{obs}}/[\text{HClO}_4]$ vs $[\text{HClO}_4]$ are shown in Supporting Information (Figure S6). The first- and second-order dependence of k_{obs} on $[\text{HClO}_4]$ suggests that PCET

occurs from the metal complexes not only to the monoprotonated iron(IV)-oxo complex ($[(\text{N4Py})\text{Fe}^{\text{IV}}(\text{OH})]^{3+}$) but also to the diprotonated iron(IV)-oxo complex ($[(\text{N4Py})\text{Fe}^{\text{IV}}(\text{OH}_2)]^{4+}$), both of which exist in equilibrium with $[(\text{N4Py})\text{Fe}^{\text{IV}}(\text{O})]^{2+}$ as shown in Scheme 1.¹⁸ It should be

Scheme 1



noted that concentrations of $[(\text{N4Py})\text{Fe}^{\text{IV}}(\text{OH})]^{3+}$ and $[(\text{N4Py})\text{Fe}^{\text{IV}}(\text{OH}_2)]^{4+}$ were too small to be detected by the change in absorption spectrum of $[(\text{N4Py})\text{Fe}^{\text{IV}}(\text{O})]^{2+}$ in the presence of large excess HClO_4 in MeCN at 298 K. This is the reason for the dependence of k_{obs} on $[\text{HClO}_4]$ (eq 2) without exhibiting any saturation behavior.

Comparison of Reactivity of C–H Bond Cleavage via PCET vs Outer-Sphere PCET. We now compare the reactivity of PCET of $[(\text{N4Py})\text{Fe}^{\text{IV}}(\text{O})]^{2+}$ in C–H bond cleavage vs outer-sphere electron-transfer in light of the Marcus theory of adiabatic electron transfer.^{34,35} The driving forces ($-\Delta G_{\text{et}}$) of PCET are obtained from the one-electron oxidation potentials (E_{ox}) of electron donors (toluene derivatives and coordinatively saturated metal complexes) and the one-electron reduction potentials (E_{red}) of $[(\text{N4Py})\text{Fe}^{\text{IV}}(\text{O})]^{2+}$ in the presence of HClO_4 as given by eq 7, where e is the elementary charge. The E_{red} values are shifted to a positive direction with increasing concentration of HClO_4 according to the Nernst equation (eq 8),¹⁹ where K_1 and K_2 are the binding constants of HClO_4 to produce the monoprotonated and diprotonated iron(III)-oxo complexes, respectively.¹⁸

$$-\Delta G_{\text{et}} = e(E_{\text{red}} - E_{\text{ox}}) \quad (7)$$

$$E_{\text{red}} = E_{\text{red}}^0 + RT \ln(K_1[\text{HClO}_4] + K_2[\text{HClO}_4]^2) \quad (8)$$

Because the E_{red} values vary depending on $[\text{HClO}_4]$ (eq 8) and the one-electron reduction potential of $[\text{Fe}^{\text{IV}}(\text{O})(\text{N4Py})]^{2+}$ was determined in the presence of 10 mM HClO_4 in MeCN at 298 K previously,¹⁹ we have chosen the conditions of 10 mM of HClO_4 (70%) to compare the driving force dependence of logarithm of the rate constants (k_{et}) of PCET reactions of $[(\text{N4Py})\text{Fe}^{\text{IV}}(\text{O})]^{2+}$ with coordinatively saturated metal complexes and those (k_{obs}) with toluene derivatives. At this concentration, electron transfer from electron donors to the monoprotonated iron(IV)-oxo complex is the major pathway as compared with the electron transfer to the diprotonated iron(IV)-oxo complex. Figure 6 shows the driving force ($-\Delta G_{\text{et}}$) dependence of $\log k_{\text{et}}$ of PCET of outer-sphere reductants (coordinatively saturated metal complexes) and $\log k_{\text{obs}}$ of PCET of toluene derivatives to $[(\text{N4Py})\text{Fe}^{\text{IV}}(\text{OH})]^{3+}$.

In the case of outer-sphere PCET from the coordinatively saturated metal complexes to $[(\text{N4Py})\text{Fe}^{\text{IV}}(\text{OH})]^{3+}$ in the presence of HClO_4 (10 mM) in MeCN at 298 K, the driving force dependence of $\log k_{\text{et}}$ is well fitted by the Marcus equation of outer-sphere electron transfer (eq 9),³⁴ where Z is frequency factor,

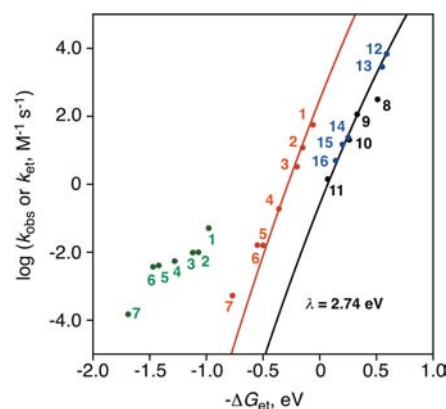


Figure 6. Plots of $\log k_{\text{obs}}$ for C–H bond cleavage of toluene derivatives ((1) hexamethylbenzene, (2) 1,2,3,4,5-pentamethylbenzene, (3) 1,2,4,5-tetramethylbenzene, (4) 1,2,4-trimethylbenzene, (5) 1,2-dimethylbenzene, (6) 1,3,5-trimethylbenzene, and (7) toluene) by $[(\text{N4Py})\text{Fe}^{\text{IV}}(\text{O})]^{2+}$ in the presence of HClO_4 (70%, 10 mM) in MeCN at 298 K vs the driving force of electron transfer ($-\Delta G = e(E_{\text{red}} - E_{\text{ox}})$) from toluene derivatives to $[(\text{N4Py})\text{Fe}^{\text{IV}}(\text{O})]^{2+}$ in the absence (green closed circles) and presence of HClO_4 (10 mM) (red closed circles). The black closed circles show the driving force dependence of the rate constants ($\log k_{\text{et}}$) of PCET from one-electron reductants ((8) $[\text{Fe}^{\text{II}}(\text{Me}_2\text{bpy})_3](\text{PF}_6)_2$, (9) $[\text{Ru}^{\text{II}}(\text{Me}_2\text{bpy})_3](\text{PF}_6)_2$, (10) $[\text{Fe}^{\text{II}}(\text{Clphen})_3](\text{PF}_6)_2$ and (11) $[\text{Ru}^{\text{II}}(\text{Clphen})_3](\text{PF}_6)_2$) to $[(\text{N4Py})\text{Fe}^{\text{IV}}(\text{O})]^{2+}$ in the presence of HClO_4 (10 mM) in MeCN at 298 K (see Table S1 in SI).¹⁹ The blue closed circles show the driving force dependence of the rate constants ($\log k_{\text{et}}$) of electron transfer from one-electron reductants ((12) decamethylferrocene, (13) octamethylferrocene, (14) 1,1'-dimethylferrocene, (15) *n*-amylferrocene and (16) ferrocene) to $[(\text{N4Py})\text{Fe}^{\text{IV}}(\text{O})]^{2+}$ in the absence of HClO_4 in MeCN at 298 K.²⁵ The black line is drawn using eq 9 with $\lambda = 2.74$ eV. The red line is drawn in parallel with the black line.

$$k_{\text{et}} = Z \exp[-(\lambda/4)(1 + \Delta G_{\text{et}}/\lambda)^2/k_B T] \quad (9)$$

which corresponds to $(k_B T K/h)$; k_B is the Boltzmann constant, T is absolute temperature, K is the formation constant of the precursor complex and h is the Planck constant) and λ is the reorganization energy of electron transfer. The Z value of outer-sphere electron-transfer reactions of coordinatively saturated metal complexes is normally taken as $1.0 \times 10^{11} \text{ M}^{-1} \text{ s}^{-1}$.^{36–39} This result indicates that the K value of outer-sphere electron-transfer reactions is as small as 0.020 M^{-1} , because there is little interaction in the precursor complex for outer-sphere electron transfer. The fitting of the data of outer-sphere PCET from the metal complexes to $[(\text{N4Py})\text{Fe}^{\text{IV}}(\text{OH})]^{3+}$ affords the λ value of 2.74 eV (black circles in Figure 6). When the k_{et} values of the outer-sphere electron-transfer reactions (coordinatively saturated metal complexes) are compared with those of toluene derivatives in the absence of HClO_4 , the latter values (green circles in Figure 6) are much larger than those expected from the outer-sphere electron transfer because the hydrogen atom transfer pathway involves much larger interactions between toluene derivatives and $[(\text{N4Py})\text{Fe}^{\text{IV}}(\text{O})]^{2+}$.

In the presence of HClO_4 (10 mM), however, the $\log k_{\text{obs}}$ values of oxidation of toluene derivatives with $[(\text{N4Py})\text{Fe}^{\text{IV}}(\text{O})]^{2+}$ (red circles in Figure 6) exhibit a parallel relationship with the driving force dependence of $\log k_{\text{et}}$ on $-\Delta G_{\text{et}}$ (black circles in Figure 6) although the k_{obs} values are always three-orders of magnitude larger than the k_{et} values. The exception is the point No. 7 (toluene), which is deviated from the red line. The reason will be discussed later. The parallel

driving force dependence of $\log k_{\text{obs}}$ with $\log k_{\text{et}}$ in Figure 6 suggests that oxidation of toluene derivatives with $[(\text{N4Py})\text{Fe}^{\text{IV}}(\text{O})]^{2+}$ in the presence of HClO_4 proceeds via PCET from toluene derivatives to $[(\text{N4Py})\text{Fe}^{\text{IV}}(\text{OH})]^{3+}$. In such a case, the difference in the k_{obs} and k_{et} values at the same driving force may result from the difference in the K values of precursor complexes (vide infra).

In order to determine the equilibrium constants of precursor complexes prior to PCET from toluene derivatives to $[(\text{N4Py})\text{Fe}^{\text{IV}}(\text{OH})]^{3+}$, the dependence of pseudo-first-order constants (k_f) on concentrations of toluene derivatives was examined using larger concentrations. An example of dependence of k_f on concentration of a toluene derivative is shown in Figure 7, where the k_f value increases with increasing

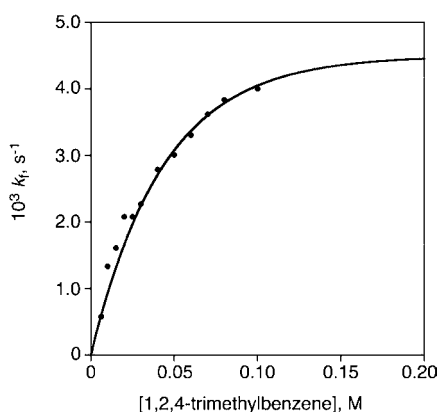


Figure 7. Plot of concentration of 1,2,4-trimethylbenzene vs first-order rate constant (k_f) in the reaction of $[(\text{N4Py})\text{Fe}^{\text{IV}}(\text{O})]^{2+}$ (0.25 mM) with 1,2,4-trimethylbenzene in the presence of 10 mM of HClO_4 in MeCN at 298 K.

concentration of 1,2,4-trimethylbenzene to approach a constant value. Such a saturation behavior of k_f on concentration of a toluene derivative is given by eq 10, where k_{ET} is the rate constant in the precursor complex, K is the formation constant of the precursor complex, and $[S]$ is concentration of a substrate.⁴⁰ Equation 10 is rewritten by eq 11, which predicts a linear correlation between k_f^{-1} vs $[S]^{-1}$. Other toluene derivatives show a similar behavior.

$$k_f = k_{\text{ET}}K[S]/(1 + K[S]) \quad (10)$$

$$k_f^{-1} = (k_{\text{ET}}K[S])^{-1} + k_{\text{ET}}^{-1} \quad (11)$$

The k_{ET} and K values were determined from linear plot of k_f^{-1} vs $[S]^{-1}$ (Figures S8 and S9 in SI). The slope and intercept to be $(4.5 \pm 0.2) \times 10^{-3} \text{ s}^{-1}$ and $(3.6 \pm 0.2) \times 10 \text{ M}^{-1}$, respectively. The k_{ET} and K values were also determined at various temperatures. The heat of formation and entropy of the precursor complex (ΔH and ΔS) were determined to be $\Delta H = -2.4 \text{ kcal mol}^{-1}$ and $\Delta S = -17 \text{ cal K}^{-1} \text{ mol}^{-1}$ from the van't Hoff plot as shown in Figure 8 (see also Figure S10 in SI). The K , ΔH and ΔS values of another toluene derivative in temperature were also determined and their values are listed in Table 2. The large K and $-\Delta H$ values in Table 2 indicate that PCET proceeds via precursor complexes in which interactions between toluene derivatives and $[(\text{N4Py})\text{Fe}^{\text{IV}}(\text{OH})]^{3+}$ are much stronger than the case of coordinatively saturated metal complexes.

As shown in Table 2, the K values of precursor complexes in PCET from toluene derivatives to $[(\text{N4Py})\text{Fe}^{\text{IV}}(\text{OH})]^{3+}$ are

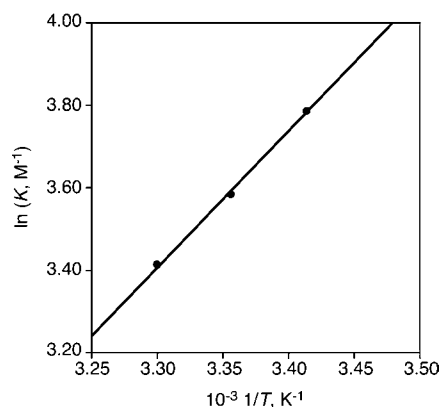


Figure 8. Plot of $\ln K$ vs $1/T$ in temperature in the reaction of $[(\text{N4Py})\text{Fe}^{\text{IV}}(\text{O})]^{2+}$ (0.25 mM) with 1,2,4-trimethylbenzene in the presence of 10 mM of HClO_4 in MeCN. The ΔH and ΔS values can be determined by van't Hoff equation, $\ln K = -\Delta H/RT + \Delta S/R$.

generally three-order of magnitude larger than the value (0.020 M^{-1}) usually used for outer-sphere electron-transfer reactions. Formation of such strong precursor complexes has also been reported for toluene derivatives with photoexcited quinones in photoinduced electron-transfer reactions.⁴¹ The charge-transfer interactions may be responsible for the binding between toluene derivatives and photoexcited quinones. There are also many examples for formation of intermediate charge-transfer complexes in organic and inorganic redox reactions.^{42–50}

Now that K values are determined, comparison of the $\log k_{\text{ET}}$ values (first-order rate constants in the precursor complexes) are made between electron transfer reactions from coordinatively saturated metal complexes and toluene derivatives to $[(\text{N4Py})\text{Fe}^{\text{IV}}(\text{OH})]^{3+}$ by using average K values of toluene derivatives (83 M^{-1}) and the value (0.020 M^{-1}) of outer-sphere electron-transfer reactions. The two separate correlations in Figure 6 are now unified as a single correlation between $\log k_{\text{ET}}$ vs $-\Delta G_{\text{et}}$ in Figure 9. Such a unified correlation together with the absence of KIE in Figure 3b strongly indicates that C–H bond cleavage of toluene derivatives by $[(\text{N4Py})\text{Fe}^{\text{IV}}(\text{O})]^{2+}$ with HClO_4 proceeds via PCET from toluene derivatives to $[(\text{N4Py})\text{Fe}^{\text{IV}}(\text{OH})]^{3+}$ through strong precursor complexes formed between toluene derivatives and $[(\text{N4Py})\text{Fe}^{\text{IV}}(\text{OH})]^{3+}$ as shown in Scheme 2.⁵⁰ The formation of strong precursor complexes prior to electron transfer in Scheme 2 suggests occurrence of an inner-sphere electron transfer pathway rather than an outer-sphere pathway.^{51,52} However, the single and unified correlation between $\log k_{\text{ET}}$ and ΔG_{et} in Figure 9, which is well fitted by the Marcus equation (eq 9), indicates that electron transfer from toluene derivatives to $[(\text{N4Py})\text{Fe}^{\text{IV}}(\text{OH})]^{3+}$ in the precursor complexes occurs in an outer-sphere pathway as the case of outer-sphere reductants (coordinatively saturated metal complexes).⁵² The absence of the second-order dependence of k_{obs} on $[\text{HClO}_4]$ in PCET from toluene derivatives may result from the much smaller interaction between toluene derivatives and the diprotonated iron(IV)-oxo complex ($[(\text{N4Py})\text{Fe}^{\text{IV}}(\text{OH}_2)]^{4+}$) due to the steric effect of second proton bound to the Fe(IV)-oxo complex.⁵³ A slight deviation from the unified line is observed for No. 7 (toluene) in Figure 9 as well as in Figure 6, because toluene may be on the borderline between the hydrogen atom transfer and PCET.

Table 2. Formation Constants and Activation Parameters in Temperature in Oxidation Reaction of Toluene Derivatives, 1,2,4-Trimethylbenzene and 1,2,4,5-Tetramethylbenzene, by $[(\text{N4Py})\text{Fe}^{\text{IV}}(\text{O})]^{2+}$ in the Presence of HClO_4 (10 mM) in MeCN

toluene derivative	formation constant (K , M^{-1})		
	303 K	298 K	293 K
1,2,4-trimethylbenzene	$(4.4 \pm 0.2) \times 10$	$(3.6 \pm 0.2) \times 10$	$(3.0 \pm 0.2) \times 10$
1,2,4,5-tetramethylbenzene	$(6.5 \pm 0.3) \times 10$	$(1.3 \pm 0.2) \times 10^2$	$(1.6 \pm 0.2) \times 10^2$
toluene derivative	ΔH (kcal mol^{-1}) ^a	ΔS (cal $\text{K}^{-1} \text{mol}^{-1}$) ^a	ΔG (eV) ^a
1,2,4-trimethylbenzene	-1.6 (± 0.1)	-15 (± 1)	0.19 (± 0.01)
1,2,4,5-tetramethylbenzene	-2.4 (± 0.2)	-17 (± 1)	0.22 (± 0.01)

^aAll of the values calculated by van't Hoff equation, $\ln K = -\Delta H/RT + \Delta S/R$.

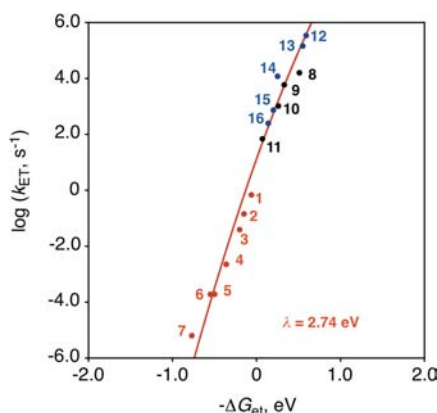
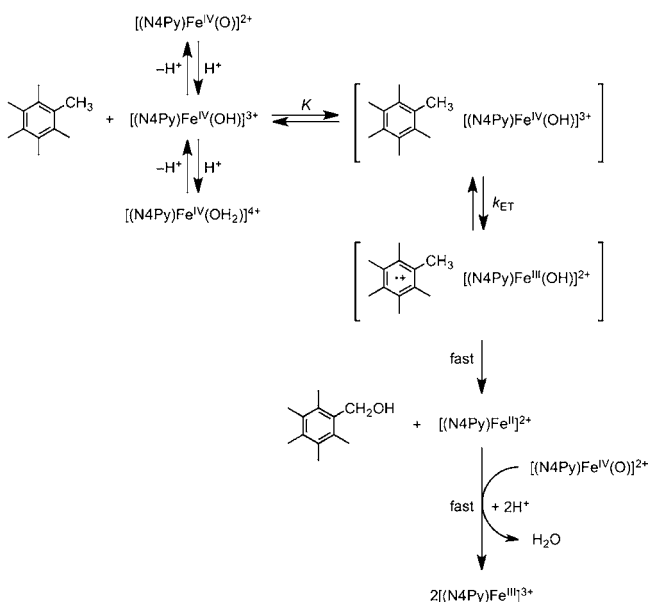


Figure 9. Plots of $\log k_{\text{ET}}$ for C–H cleavage of toluene derivatives by $[(\text{N4Py})\text{Fe}^{\text{IV}}(\text{O})]^{2+}$ in the presence of HClO_4 (70%, 10 mM) in MeCN at 298 K vs the driving force of electron transfer $[-\Delta G = e(E_{\text{red}} - E_{\text{ox}})]$ from toluene derivatives to $[(\text{N4Py})\text{Fe}^{\text{IV}}(\text{O})]^{2+}$ in the presence of HClO_4 (10 mM) (red closed circles). The black closed circles show the driving force dependence of the rate constants ($\log k_{\text{ET}}$) of PCET from one-electron reductants to $[(\text{N4Py})\text{Fe}^{\text{IV}}(\text{O})]^{2+}$ in the presence of HClO_4 (10 mM) in MeCN at 298 K ($k_{\text{ET}} = k_{\text{et}}/K$, $K = 0.020$). The red line is drawn based on eq 9 with $\lambda = 2.74$ eV.¹⁹ The blue closed circles show the driving force dependence of the rate constants ($\log k_{\text{ET}}$) of electron transfer from one-electron reductants to $[(\text{N4Py})\text{Fe}^{\text{IV}}(\text{O})]^{2+}$ in the absence of HClO_4 in MeCN at 298 K.²⁵ The numberings of substrates denote those used in Figure 6.

Scheme 2



CONCLUSION

C–H bond cleavage of toluene derivatives by a nonheme iron(IV)-oxo complex, $[(\text{N4Py})\text{Fe}^{\text{IV}}(\text{O})]^{2+}$, is remarkably enhanced by Brønsted acid (HClO_4) to yield benzyl alcohol derivatives and $[(\text{N4Py})\text{Fe}^{\text{III}}(\text{OH}_2)]^{3+}$ in MeCN at 298 K. Even toluene, which has high oxidation potential (2.20 V vs SCE), can be oxidized efficiently by $[(\text{N4Py})\text{Fe}^{\text{IV}}(\text{O})]^{2+}$ in the presence of HClO_4 . Such a remarkable acceleration of C–H bond cleavage of toluene derivatives with $[(\text{N4Py})\text{Fe}^{\text{IV}}(\text{O})]^{2+}$ in the presence of HClO_4 results from the change in the reaction mechanism from direct hydrogen atom transfer from toluene derivatives to $[(\text{N4Py})\text{Fe}^{\text{IV}}(\text{O})]^{2+}$ in the absence of HClO_4 to PCET from toluene derivatives to $[(\text{N4Py})\text{Fe}^{\text{IV}}(\text{OH})]^{3+}$ in the presence of HClO_4 via strong precursor complexes formed between toluene derivatives and $[(\text{N4Py})\text{Fe}^{\text{IV}}(\text{OH})]^{3+}$ as indicated by the unified correlation of $\log k_{\text{ET}}$ vs the PCET deriving force ($-\Delta G_{\text{et}}$) in light of the Marcus theory of outer-sphere electron transfer and the absence of KIE. In the case of toluene, which is the least reactive, the hydrogen atom transfer pathway competes with the PCET pathway to exhibit a small KIE (2.0), and the k_{obs} value is a bit larger than that expected from the outer-sphere electron transfer (no. 7 in Figure 6).

EXPERIMENTAL SECTION

Materials. All chemicals, which were the best available purity, were purchased from Aldrich Chemical Co. and Tokyo Chemical Industry, used without further purification unless otherwise noted. Solvents, such as acetonitrile (MeCN) and diethyl ether, were dried according to the literature procedures and distilled under Ar prior to use.⁵⁴ Nonheme iron(II) complex $[(\text{N4Py})\text{Fe}^{\text{II}}(\text{MeCN})_2](\text{ClO}_4)_2$ and its corresponding iron(IV)-oxo $[(\text{N4Py})\text{Fe}^{\text{IV}}(\text{O})]^{2+}$ were prepared by the literature methods.^{15,55} Iodosylbenzene (PhIO) was prepared by the literature method.⁵⁶ Perchloric acid (70 wt % in H_2O) was purchased from Sigma Aldrich Chemical Co.

Caution: Perchlorate salts are potentially explosive and should be handled with care.

Kinetic Studies. Kinetic measurements were performed on a Hewlett-Packard 8453 photodiode-array spectrophotometer using a 10 mm quartz cuvette (10 mm path length) at 298 K. C–H bond cleavage of toluene derivatives by $[(\text{N4Py})\text{Fe}^{\text{IV}}(\text{O})]^{2+}$ was examined by monitoring the spectral change due to $[(\text{N4Py})\text{Fe}^{\text{IV}}(\text{O})]^{2+}$ (2.5×10^{-5} M) with various concentrations of alkylbenzenes (2.5×10^{-3} – 1.0×10^{-1} M) in the absence and presence of HClO_4 in MeCN at 298 K. Rates of C–H bond cleavage of toluene derivatives by $[(\text{N4Py})\text{Fe}^{\text{IV}}(\text{O})]^{2+}$ were monitored by the decay of the absorption band at 695 nm due to $[(\text{N4Py})\text{Fe}^{\text{IV}}(\text{O})]^{2+}$ ($\lambda_{\text{max}} = 695$ nm) in the absence and presence of HClO_4 in MeCN. The concentration of toluene derivatives was maintained at least more than 10-fold excess of $[(\text{N4Py})\text{Fe}^{\text{IV}}(\text{O})]^{2+}$ to attain pseudofirst-order conditions. First-order fitting of the kinetic data allowed us to determine the pseudofirst-order rate constants. The first-order plots were linear for three or more half-lives with the correlation coefficient $\rho > 0.999$. In each case, it was

confirmed that the rate constants derived from at least five independent measurements agreed within an experimental error of $\pm 5\%$. The pseudofirst-order rate constants increased proportionally with increase in concentrations of substrates, from which second-order rate constants were determined.

Product Analysis. Typically, hexamethylbenzene (2.0×10^{-2} M) was added to a MeCN solution (0.50 mL) containing $[(\text{N4Py})\text{Fe}^{\text{IV}}(\text{O})]^{2+}$ (4.0×10^{-3} M) in the presence of HClO_4 (10 mM) in a vial. The reaction was complete within 5 min under these conditions. Products formed in the oxidation reactions of toluene derivatives by $[(\text{N4Py})\text{Fe}^{\text{IV}}(\text{O})]^{2+}$, which were carried out in the presence of HClO_4 under Ar atmosphere in MeCN- d_3 at 298 K, were analyzed by ^1H NMR. Quantitative analyses were made on the basis of comparison of ^1H NMR spectral integration between products and their authentic samples. In the case of hexamethylbenzene, pentamethyl benzyl alcohol was obtained as a product with 50% of yield (based on the intermediate generated) in the presence of HClO_4 (10 mM). In the cases of other toluene derivatives, (methyl) $_n$ benzene, (methyl) $_n$ benzyl alcohols were obtained in quantitative amounts^{17,31} by ^1H NMR, as the case of hexamethylbenzene (HMB).

Instrumentation. UV-vis spectra were recorded on a Hewlett-Packard 8453 photodiode-array spectrophotometer. X-band EPR spectra were taken at 5 K using a X-band Bruker EMX-plus spectrometer equipped with a dual mode cavity (ER 4116DM). Low temperatures were achieved and controlled with an Oxford Instruments ESR900 liquid He quartz cryostat with an Oxford Instruments ITC503 temperature and gas flow controller. The experimental parameters for EPR spectra were as follows: Microwave frequency = 9.648 GHz, microwave power = 1 mW and modulation amplitude = 10 G. ^1H NMR spectra were measured with Bruker model digital AVANCE III 400 FT-NMR spectrometer. GC-MS spectra were monitored using a Shimadzu GC-17A gas chromatograph and Shimadzu MS-QP5000 mass spectrometer.

■ ASSOCIATED CONTENT

● Supporting Information

Table S1 and Figures S1–S10. This material is available free of charge via the Internet at <http://pubs.acs.org>.

■ AUTHOR INFORMATION

Corresponding Author

fukuzumi@chem.eng.osaka-u.ac.jp; wwnam@ewha.ac.kr

Notes

The authors declare no competing financial interest.

■ ACKNOWLEDGMENTS

The research at OU was supported by Grant-in-Aid (No. 19205019 to S.F.) and Global COE program, “the Global Education and Research Center for Bio-Environmental Chemistry” from the Ministry of Education, Culture, Sports, Science and Technology, Japan (to S.F.). The research at EWU was supported by NRF/MEST of Korea through CRI (to W.N.), GRL (2010-00353) (to W.N.), 2011 KRICT OASIS project (to W.N.), and WCU (R31-2008-000-10010-0) (to W.N. and S.F.). J.P. gratefully acknowledges support from JSPS by Grant-in-Aid for JSPS fellowship for young scientists.

■ REFERENCES

(1) (a) Ortiz de Montellano, P. R. *Cytochrome P450: Structure, Mechanism, and Biochemistry*, 3rd ed.; Kluwer Academic/Plenum Publishers: New York, 2005. (b) Meunier, B., Ed. *Biomimetic Oxidations Catalyzed by Transition Metal Complexes*; Imperial College Press: London, 2000. (c) *The Ubiquitous Role of Cytochrome P450 Proteins In Metal Ions in Life Sciences*; Sigel, A., Sigel, H., Sigel, R. K. O., Eds.; John Wiley & Sons Ltd: Chichester, England, 2007; Vol. 3.

(2) (a) Sono, M.; Roach, M. P.; Coulter, E. D.; Dawson, J. H. *Chem. Rev.* **1996**, *96*, 2841. (b) Watanabe, Y. *J. Biol. Inorg. Chem.* **2001**, *6*, 846. (c) Jung, C. *Biochim. Biophys. Acta* **2011**, *1814*, 46.

(3) Rohde, J.-U.; In, J.-H.; Lim, M. H.; Brennessel, W. W.; Bukowski, M. R.; Stubna, A.; Münck, E.; Nam, W.; Que, L., Jr. *Science* **2003**, *299*, 1037.

(4) (a) de Visser, S. P.; Rohde, J.-U.; Lee, Y.-M.; Cho, J.; Nam, W. *Coord. Chem. Rev.* **2013**, *257*, 381. (b) McDonald, A. R.; Que, L., Jr. *Coord. Chem. Rev.* **2013**, *257*, 414.

(5) (a) Meunier, B.; de Visser, S. P.; Shaik, S. *Chem. Rev.* **2004**, *104*, 3947. (b) Shaik, S.; Cohen, S.; Wang, Y.; Chen, H.; Kumar, D.; Thiel, W. *Chem. Rev.* **2010**, *110*, 949. (c) Abu-Omar, M. M.; Loaiza, A.; Hontzeas, N. *Chem. Rev.* **2005**, *105*, 2227. (d) Denisov, I. G.; Makris, T. M.; Sligar, S. G.; Schlichting, I. *Chem. Rev.* **2005**, *105*, 2253. (e) Ortiz de Montellano, P. R. *Chem. Rev.* **2010**, *110*, 932.

(6) (a) Groves, J. T.; Shalayaev, K.; Lee, J. In *The Porphyrin Handbook*; Kadish, K. M., Smith, K. M., Guillard, R., Eds.; Elsevier Science: New York, 2000; Vol. 4, pp 17–40. (b) Watanabe, Y. In *The Porphyrin Handbook*; Kadish, K. M., Smith, K. M., Guillard, R., Eds.; Elsevier Science: New York, 2000; Vol. 4, pp 97–117. (c) Groves, J. T. *J. Inorg. Biochem.* **2006**, *100*, 434.

(7) (a) Gunay, A.; Theopold, K. H. *Chem. Rev.* **2010**, *110*, 1060. (b) Che, C.-M.; Lo, V. K.-Y.; Zhou, C.-Y.; Huang, J.-S. *Chem. Soc. Rev.* **2011**, *40*, 1950. (c) Costas, M. *Coord. Chem. Rev.* **2011**, *255*, 2912.

(8) (a) Cho, K.; Leeladee, P.; McGown, A. J.; DeBeer, S.; Goldberg, D. P. *J. Am. Chem. Soc.* **2012**, *134*, 7392. (b) Cho, K.-B.; Chen, H.; Janardanan, D.; de Visser, S. P.; Shaik, S.; Nam, W. *Chem. Commun.* **2012**, *48*, 2189. (c) Seo, M. S.; Kim, N. H.; Cho, K.-B.; So, J. E.; Park, S. K.; Clemaney, M.; Garcia-Serres, R.; Latour, J.-M.; Shaik, S.; Nam, W. *Chem. Sci.* **2011**, *2*, 1039. (d) Borovik, A. S. *Chem. Soc. Rev.* **2011**, *40*, 1870. (e) Janardanan, D.; Wang, Y.; Schyman, P.; Que, L., Jr.; Shaik, S. *Angew. Chem., Int. Ed.* **2010**, *49*, 3342.

(9) (a) Krebs, C.; Fujimori, D. G.; Walsh, C. T.; Bollinger, J. M., Jr. *Acc. Chem. Res.* **2007**, *40*, 484. (b) Que, L., Jr. *Acc. Chem. Res.* **2007**, *40*, 493. (c) Nam, W. *Acc. Chem. Res.* **2007**, *40*, 522. (d) Borovik, A. S. *Acc. Chem. Res.* **2005**, *38*, 54. (e) Shaik, S.; Lai, W.; Chen, H.; Wang, Y. *Acc. Chem. Res.* **2010**, *43*, 1154.

(10) Hong, S.; Lee, Y.-M.; Cho, K.-B.; Sundaravel, K.; Cho, J.; Kim, M. J.; Shin, W.; Nam, W. *J. Am. Chem. Soc.* **2011**, *133*, 11876.

(11) Tang, H.; Guan, J.; Zhang, L.; Liu, H.; Huang, X. *Phys. Chem. Chem. Phys.* **2012**, *14*, 12863.

(12) Kumar, D.; Sastry, G. N.; de Visser, S. P. *J. Phys. Chem. B* **2012**, *116*, 718.

(13) (a) Groves, J. T.; McClusky, G. A. *J. Am. Chem. Soc.* **1976**, *98*, 859. (b) Ortiz de Montellano, P. R.; Stearns, R. A. *J. Am. Chem. Soc.* **1987**, *109*, 3415. (c) Schöneboom, J. C.; Cohen, S.; Lin, H.; Shaik, S.; Thiel, W. *J. Am. Chem. Soc.* **2004**, *126*, 4017. (d) Hirao, H.; Kumar, D.; Que, L., Jr.; Shaik, S. *J. Am. Chem. Soc.* **2006**, *128*, 8590.

(14) Chiavarino, B.; Cipollini, R.; Crestoni, M. E.; Fornarini, S.; Fornarini, S.; Lapi, A. *J. Am. Chem. Soc.* **2008**, *130*, 3208.

(15) Kaizer, J.; Klinker, E. J.; Oh, N. Y.; Rohde, J.-U.; Song, W. J.; Stubna, A.; Kim, J.; Münck, E.; Nam, W.; Que, L., Jr. *J. Am. Chem. Soc.* **2004**, *126*, 472.

(16) (a) Park, M. J.; Lee, J.; Suh, Y.; Kim, J.; Nam, W. *J. Am. Chem. Soc.* **2006**, *128*, 2630. (b) Sastri, C. V.; Lee, J.; Oh, K.; Lee, Y. J.; Lee, J.; Jackson, T. A.; Ray, K.; Hirao, H.; Shin, W.; Halfen, J. A.; Kim, J.; Que, L., Jr.; Shaik, S.; Nam, W. *Proc. Natl. Acad. Sci. U. S. A.* **2007**, *104*, 19181. (c) Jeong, Y. J.; Kang, Y.; Han, A.-R.; Lee, Y.-M.; Kotani, H.; Fukuzumi, S.; Nam, W. *Angew. Chem., Int. Ed.* **2008**, *47*, 7321. (d) Lee, Y.-M.; Dhuri, S. N.; Sawant, S. C.; Cho, J.; Kubo, M.; Ogura, T.; Fukuzumi, S.; Nam, W. *Angew. Chem., Int. Ed.* **2009**, *48*, 1803.

(17) (a) Lee, Y.-M.; Hong, S.; Morimoto, Y.; Shin, W.; Fukuzumi, S.; Nam, W. *J. Am. Chem. Soc.* **2010**, *132*, 10668. (b) Wilson, S. A.; Chen, J.; Hong, S.; Lee, Y.-M.; Clémancey, M.; Garcia-Serres, R.; Nomura, T.; Ogura, T.; Latour, J.-M.; Hedman, B.; Hodfson, K. O.; Nam, W.; Solomon, E. I. *J. Am. Chem. Soc.* **2012**, *134*, 11791.

(18) Fukuzumi, S. *Coord. Chem. Rev.* **2013**, DOI: 10.1016/j.ccr.2012.07.021.

- (19) Park, J.; Morimoto, Y.; Lee, Y.-M.; Nam, W.; Fukuzumi, S. *J. Am. Chem. Soc.* **2012**, *134*, 3903.
- (20) Morimoto, Y.; Park, J.; Suenobu, T.; Lee, Y.-M.; Nam, W.; Fukuzumi, S. *Inorg. Chem.* **2012**, *51*, 10025.
- (21) (a) Fukuzumi, S.; Morimoto, Y.; Kotani, H.; Naumov, P.; Lee, Y.-M.; Nam, W. *Nature Chem.* **2010**, *2*, 756. (b) Morimoto, Y.; Kotani, H.; Park, J.; Lee, Y.-M.; Nam, W.; Fukuzumi, S. *J. Am. Chem. Soc.* **2011**, *133*, 403. (c) Park, J.; Morimoto, Y.; Lee, Y.-M.; Nam, W.; Fukuzumi, S. *J. Am. Chem. Soc.* **2011**, *133*, 5236. (d) Park, J.; Morimoto, Y.; Lee, Y.-M.; You, Y.; Nam, W.; Fukuzumi, S. *Inorg. Chem.* **2011**, *50*, 11612.
- (22) Bond dissociation energy (BDE) of acetonitrile is reported to be 96 ± 1 kcal mol⁻¹,²³ which is significantly higher than those of toluene derivatives (e.g., 88.5 kcal mol⁻¹).²⁴ In addition, the oxidation potential of acetonitrile is much higher than those of toluene derivatives. Indeed [(N4Py)Fe^{IV}(O)]²⁺ is stable in the absence and presence of HClO₄ in acetonitrile.
- (23) Menon, A. S.; Henry, D. J.; Bally, T.; Radom, L. *Org. Biomol. Chem.* **2011**, *9*, 3636.
- (24) Kojima, T.; Nakayama, K.; Ikemura, K.; Ogura, T.; Fukuzumi, S. *J. Am. Chem. Soc.* **2011**, *133*, 11692.
- (25) Lee, Y.-M.; Kotani, H.; Suenobu, T.; Nam, W.; Fukuzumi, S. *J. Am. Chem. Soc.* **2008**, *130*, 434.
- (26) (a) Roelfes, G.; Vrajmasu, V.; Chen, K.; Ho, R. Y. N.; Rohde, J.-U.; Zondervan, C.; la Crois, R. M.; Schudde, E. P.; Lutz, M.; Spek, A. L.; Hage, R.; Feringa, B. L.; Münck, E.; Que, L., Jr. *Inorg. Chem.* **2003**, *42*, 2639. (b) Hong, S.; Lee, Y.-M.; Shin, W.; Fukuzumi, S.; Nam, W. *J. Am. Chem. Soc.* **2009**, *131*, 13910.
- (27) Fukuzumi, S.; Ishikawa, K.; Hironaka, K.; Tanaka, T. *J. Chem. Soc., Perkin Trans. 2* **1987**, 751.
- (28) (a) Fukuzumi, S.; Kuroda, S. *Res. Chem. Int.* **1999**, *25*, 789. (b) Fukuzumi, S.; Chiba, M.; Ishikawa, M.; Ishikawa, K.; Tanaka, T. *J. Chem. Soc., Perkin Trans. 2* **1989**, 1417. (c) Fukuzumi, S.; Ishikawa, M.; Tanaka, T. *Tetrahedron* **1986**, *42*, 1021. (d) Fukuzumi, S.; Chiba, M.; Tanaka, T. *Chem. Lett.* **1989**, 31.
- (29) Kwart, H. *Acc. Chem. Res.* **1982**, *15*, 401.
- (30) (a) Price, J. C.; Barr, E. W.; Glass, T. E.; Krebs, C.; Bollinger, J. M., Jr. *J. Am. Chem. Soc.* **2003**, *125*, 13008. (b) Wu, A.; Mayer, J. M. J. *Am. Chem. Soc.* **2008**, *130*, 14745.
- (31) (a) Kohen, A.; Klinman, J. P. *Acc. Chem. Res.* **1998**, *31*, 397. (b) Knapp, M. J.; Rickert, K.; Klinman, J. P. *J. Am. Chem. Soc.* **2002**, *124*, 3865. (c) Klinman, J. P. *Biochim. Biophys. Acta, Bioenergetics* **2006**, *1757*, 981. (d) McCusker, K. P.; Klinman, J. P. *J. Am. Chem. Soc.* **2010**, *132*, 5114.
- (32) Fukuzumi, S.; Kobayashi, T.; Suenobu, T. *J. Am. Chem. Soc.* **2010**, *132*, 1496.
- (33) Fukuzumi, S.; Ohkubo, K.; Suenobu, T.; Kato, K.; Fujitsuka, M.; Ito, O. *J. Am. Chem. Soc.* **2001**, *123*, 8459.
- (34) (a) Marcus, R. A. *Annu. Rev. Phys. Chem.* **1964**, *15*, 155. (b) Marcus, R. A. *Discuss. Faraday Soc.* **1960**, *29*, 129. (c) Marcus, R. A. *Angew. Chem., Int. Ed. Engl.* **1993**, *32*, 1111.
- (35) (a) Cannon, R. D. *Electron-Transfer Reactions*; Butterworth: London, 1980. (b) Ebersson, L. *Adv. Phys. Org. Chem.* **1982**, *18*, 79. (c) Silverstein, T. P. *J. Chem. Educ.* **2012**, *89*, 1159.
- (36) (a) Sutin, N. *Acc. Chem. Res.* **1968**, *1*, 225. (b) Sutin, N. *Adv. Chem. Phys.* **1999**, *106*, 7. (c) Chou, M.; Creutz, C.; Sutin, N. *J. Am. Chem. Soc.* **1977**, *99*, 5615. (d) Keeney, L.; Hynes, M. J. *Dalton Trans.* **2005**, 133.
- (37) (a) Fukuzumi, S.; Honda, T.; Kojima, T. *Coord. Chem. Rev.* **2012**, *256*, 2488. (b) Fukuzumi, S.; Karlin, K. D. *Coord. Chem. Rev.* **2012**, *257*, 187. (c) Tahsini, L.; Kotani, H.; Lee, Y.-M.; Cho, J.; Nam, W.; Karlin, K. D.; Fukuzumi, S. *Chem.–Eur. J.* **2012**, *18*, 1084. (d) Yoon, H.; Morimoto, Y.; Lee, Y.-M.; Nam, W.; Fukuzumi, S. *Chem. Commun.* **2012**, *48*, 11187.
- (38) (a) Takai, A.; Gros, C. P.; Barbe, J.-M.; Guilard, R.; Fukuzumi, S. *Chem.–Eur. J.* **2009**, *15*, 3110. (b) Nakanishi, T.; Ohkubo, K.; Kojima, T.; Fukuzumi, S. *J. Am. Chem. Soc.* **2009**, *131*, 577. (c) Murakami, M.; Ohkubo, K.; Fukuzumi, S. *Chem.–Eur. J.* **2010**, *16*, 7820.
- (39) (a) Fukuzumi, S.; Nakanishi, I.; Tanaka, K.; Suenobu, T.; Tabard, A.; Guilard, R.; Van Caemelbecke, E.; Kadish, K. M. *J. Am. Chem. Soc.* **1999**, *121*, 785. (b) Fukuzumi, S.; Mochizuki, S.; Tanaka, T. *Inorg. Chem.* **1989**, *28*, 2459.
- (40) The saturation behavior could be interpreted as an acid-substrate complexation. However, it was confirmed that no protonation of TMB occurred in the presence of HClO₄ up to 20 mM (see Figure S7 in SI). Thus, the observed saturation behavior results from a strong precursor complex rather than the protonation of the substrate.
- (41) Hubig, S. M.; Kochi, J. K. *J. Am. Chem. Soc.* **1999**, *121*, 1688.
- (42) (a) Fukuzumi, S.; Mochida, K.; Kochi, J. K. *J. Am. Chem. Soc.* **1979**, *101*, 5961. (b) Fukuzumi, S.; Kochi, J. K. *J. Am. Chem. Soc.* **1980**, *102*, 2141. (c) Fukuzumi, S.; Kochi, J. K. *J. Am. Chem. Soc.* **1981**, *103*, 2783. (d) Fukuzumi, S.; Kochi, J. K. *J. Am. Chem. Soc.* **1981**, *103*, 7240. (e) Fukuzumi, S.; Kochi, J. K. *J. Am. Chem. Soc.* **1982**, *104*, 7599.
- (43) (a) Park, J. S.; Karnas, E.; Ohkubo, K.; Chen, P.; Kadish, K. M.; Fukuzumi, S.; Bielawski, C. W.; Hudnall, T. W.; Lynch, V. M.; Sessler, J. L. *Science* **2010**, *329*, 1324. (b) Fukuzumi, S.; Ohkubo, K.; Kawashima, Y.; Kim, D. S.; Park, J.-S.; Jana, A.; Lynch, V. M.; Kim, D.-H.; Sessler, J. L. *J. Am. Chem. Soc.* **2011**, *133*, 15938.
- (44) (a) Fukuzumi, S.; Kochi, J. K. *Tetrahedron* **1982**, *38*, 1035. (b) Kim, J. H.; Lindeman, S. V.; Kochi, J. K. *J. Am. Chem. Soc.* **2001**, *123*, 4951. (c) Fukuzumi, S.; Koumitsu, S.; Hironaka, K.; Tanaka, T. *J. Am. Chem. Soc.* **1987**, *109*, 305. (d) Fukuzumi, S.; Nishizawa, N.; Tanaka, T. *J. Org. Chem.* **1984**, *49*, 3571.
- (45) (a) Zaman, K. M.; Yamamoto, S.; Nishimura, N.; Maruta, J.; Fukuzumi, S. *J. Am. Chem. Soc.* **1994**, *116*, 12099. (b) Zhu, X.-Q.; Zhang, J.-Y.; Cheng, J.-P. *J. Org. Chem.* **2006**, *71*, 7007. (c) Fukuzumi, S.; Endo, Y.; Imahori, H. *J. Am. Chem. Soc.* **2002**, *124*, 10974. (d) Zhu, X.-Q.; Li, X.-T.; Han, S.-H.; Mei, L.-R. *J. Org. Chem.* **2012**, *77*, 4774.
- (46) (a) Fukuzumi, S.; Ohkubo, K.; Tokuda, Y.; Suenobu, T. *J. Am. Chem. Soc.* **2000**, *122*, 4286. (b) Lu, Y.; Zhao, Y.; Handoo, K. L.; Parker, V. D. *Org. Biomol. Chem.* **2003**, *1*, 173. (c) Ohkubo, K.; Fukuzumi, S. *J. Phys. Chem. A* **2005**, *109*, 1105. (d) Le Magueres, P.; Lindeman, S. V.; Kochi, J. K. *Organometallics* **2001**, *20*, 115.
- (47) Kochi, J. K. *Acc. Chem. Res.* **1992**, *25*, 39.
- (48) Goodwin, J. A.; Wilson, L. J.; Stanbury, D. M.; Scott, R. A. *Inorg. Chem.* **1988**, *28*, 42.
- (49) (a) Rosokha, S. V.; Kochi, J. K. *Acc. Chem. Res.* **2008**, *41*, 641. (b) Hubig, S. M.; Kochi, J. K. *J. Am. Chem. Soc.* **1999**, *121*, 1688. (c) Gaede, W.; van Eldik, R. *Inorg. Chem.* **1994**, *33*, 2204.
- (50) The saturation behavior of k_f vs concentration of a substrate may result from the competition between deprotonation of [(N4Py)Fe^{IV}(OH)]³⁺ and the reaction with the substrate. In such a case, the rate-determining step at the saturated would be the protonation of [(N4Py)Fe^{IV}(O)]²⁺, when the rate constant would be independent of the PCET driving force. The results in Figure 9, which exhibit a single correlation between log k_{ET} vs $-\Delta G_{et}$, clearly indicate that the saturation behavior in Figure 7 does not result from the change in the rate-determining step to the protonation of [(N4Py)Fe^{IV}(O)]²⁺.
- (51) For the classical definition of inner-sphere electron transfer, see: (a) Taube, H.; Myers, H. J.; Rich, R. L. *J. Am. Chem. Soc.* **1953**, *75*, 4118. (b) Taube, H. *Science* **1984**, *226*, 1028.
- (52) For more generalized distinction between the inner-sphere and outer-sphere electron-transfer pathways, see: (a) Rosokha, S. V.; Kochi, J. K. *Acc. Chem. Res.* **2008**, *41*, 641. (b) Fukuzumi, S.; Wong, C. L.; Kochi, J. K. *J. Am. Chem. Soc.* **1980**, *102*, 2928. (c) Fukuzumi, S.; Kochi, J. K. *Bull. Chem. Soc. Jpn.* **1983**, *56*, 969.
- (53) The assumption that all reactivities at 10 mM HClO₄ are dominated by the monoprotinated species [(N4Py)Fe^{IV}(OH)]³⁺ is valid for oxidation of toluene derivatives with [Fe^{IV}(O)(N4Py)]²⁺ as indicated by linear correlations between the k_{obs} values and HClO₄ concentration in Figure 2. In the case of PCET from inorganic one-electron reductants to [Fe^{IV}(O)(N4Py)]²⁺, however, the diprotinated species [(N4Py)Fe^{IV}(OH)₂]⁴⁺ may also be involved as indicated by the contribution of the second-order dependence of k_{obs} on [HClO₄] in Figure 5. At 10 mM HClO₄, there is some contribution of [(N4Py)Fe^{IV}(OH)₂]⁴⁺ in PCET from inorganic one-electron reductants to

$[\text{Fe}^{\text{IV}}(\text{O})(\text{N4Py})]^{2+}$. This may be the reason why the k_{ET} values of PCET oxidation of toluene derivatives (red points) are somewhat smaller than the Marcus line in Figure 9. Nevertheless, the assumption that all reactivities at 10 mM HClO_4 are dominated by the monoprotonated species ($[(\text{N4Py})\text{Fe}^{\text{IV}}(\text{OH})]^{3+}$) is good enough to obtain the largely unified correlation in Figure 9.

(54) Armarego, W. L. F.; Chai, C. L. L. *Purification of Laboratory Chemicals*, 6th ed.; Pergamon Press: Oxford, 2009.

(55) Lubben, M.; Meetsma, A.; Wilkinson, E. C.; Feringa, B.; Que, L., Jr. *Angew. Chem., Int. Ed.* **1995**, *34*, 1512.

(56) *Organic Syntheses*; Saltzman, H., Sharefkin, J. G., Eds.; Wiley: New York, 1973; Vol. V, p 658.